JACS
JOURNAL OF THE AMERICAN CHEMICAL SOCIETY
Article
pubs.acs.org/JACS

The Elusive 5′-Deoxyadenosyl Radical in Coenzyme-B_{12}-Mediated Reactions

Denis Bucher,*[,†,⊥] Gregory M. Sandala,*[,†,‡] Bo Durbeej,[§] Leo Radom,*[,†] and David M. Smith*[,‡,∥]

[†]School of Chemistry and ARC Centre of Excellence for Free Radical Chemistry and Biotechnology, University of Sydney, Sydney, NSW 2006, Australia

[‡]Division of Organic Chemistry and Biochemistry, Ruđer Bošković Institute, 10002 Zagreb, Croatia

[§]Division of Computational Physics, IFM Theory and Modelling, Linköping University, SE-581 83 Linköping, Sweden

[∥]Computer-Chemie-Centrum, University of Erlangen-Nürnberg, 91052 Erlangen, Germany

Supporting Information

ABSTRACT: Vitamin B_{12} and its biologically active counterparts possess the only examples of carbon−cobalt bonds in living systems. The role of such motifs as radical reservoirs has potential application in future catalytic and electronic nanodevices. To fully understand radical generation in coenzyme B_{12} (dAdoCbl)-dependent enzymes, however, major obstacles still need to be overcome. In this work, we have used Car−Parrinello molecular dynamics (CPMD) simulations, in a mixed quantum mechanics/molecular mechanics (QM/MM) framework, to investigate the initial stages of the methylmalonyl-CoA-mutase-catalyzed reaction. We demonstrate that the 5′-deoxyadenosyl radical (dAdo•) exists as a distinct entity in this reaction, consistent with the results of extensive experimental and some previous theoretical studies. We report free energy calculations and first-principles trajectories that help understand how B_{12} enzymes catalyze coenzyme activation and control highly reactive radical intermediates.

INTRODUCTION

Derivatives of vitamin B_{12} participate in a variety of physiological pathways that are essential to life, including energy generation and DNA synthesis and regulation.[1] The reactions dependent on coenzyme B_{12} (or 5′-deoxyadenosylcobalamin, dAdoCbl) rely on radical intermediates to interchange a hydrogen atom and functional group on adjacent carbons.[2−7] As such, coenzyme B_{12} is often described as a "free radical reservoir" because homolysis of its extraordinary Co−C5′ bond leads to the highly reactive dAdo• radical intermediate. Impressively, dAdoCbl-dependent enzymes enhance the rate of Co−C5′ bond homolysis by up to a trillion-fold relative to solution, in what is almost certainly one of nature's most efficient and well-regulated mechanisms.[8] In this context, we can identify two important questions related to the initial stages of the dAdoCbl-dependent reactions. The first relates to the origin of the ∼70 kJ mol^{-1} reduction in the barrier for Co−C5′ cleavage achieved by the enzyme[9] and the detailed role of the protein in this step. The second, related, question concerns the formation of the highly reactive dAdo• species, its lifetime under thermolytic conditions and its interaction with the enzyme. Understanding the origin of these effects should help to demonstrate how enzymes exert strict control over radical chemistry, and may reveal useful strategies from which to develop novel technologies, such as biomimetic nanoelectronic devices.[10]

Methylmalonyl-CoA mutase (MCM) is arguably the most extensively characterized member of the dAdoCbl-dependent family and is an ideal candidate to scrutinize the dramatic catalysis because of the availability of high-resolution crystal structures[11,12] and a large collection of experimental and computational data.[13] Found in bacteria and mammals, MCM catalyzes the reversible interconversion of methylmalonyl CoA (**1**) and succinyl CoA (**2**).

(1) (2)

The inability of MCM to execute this step leads to the potentially fatal disease methylmalonic acidemia, an inborn error of metabolism characterized by excessive levels of methylmalonyl CoA.[14]

The generally accepted mechanism of the initial stages of the dAdoCbl-dependent reactions, including that of MCM, proceeds via a stepwise pathway (Figure 1a) involving Co−C5′ homolysis (step I) and H-atom transfer (step II), with dAdo• as a distinct intermediate.[3,5] Selected relevant studies that support this pathway include isotope labeling experiments[15,16] and EPR measurements involving the naturally occurring cofactor (AdoCbl)[17−20] and a synthetic analogue (3′,4′-anhydro-dAdoCbl).[21,22] For the specific case of MCM, it

Received: August 17, 2011
Published: January 6, 2012

   dx.doi.org/10.1021/ja207809b | J. Am. Chem.Soc. 2012, 134, 1591−1599

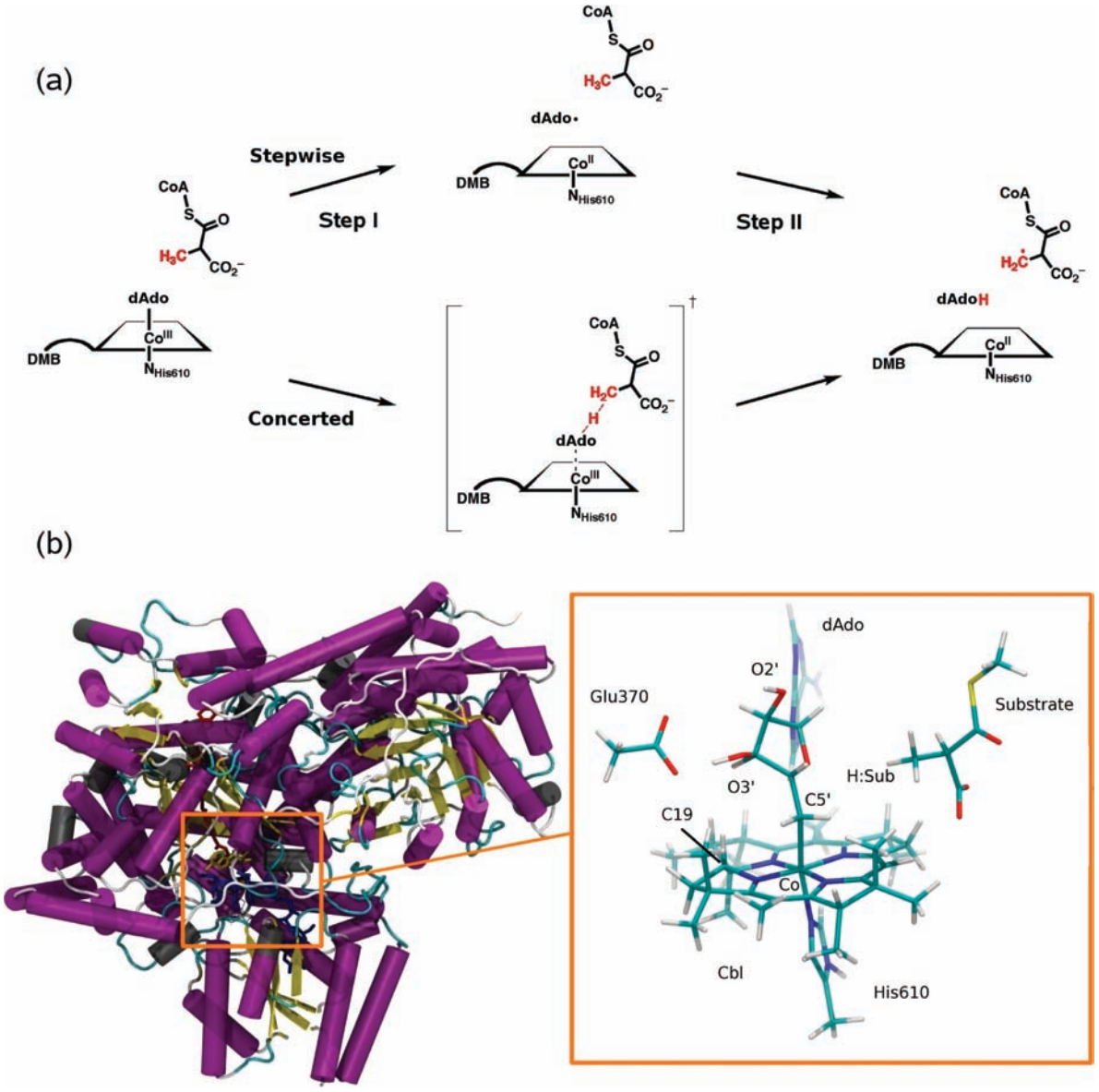

Figure 1. Two possible pathways and the active site for the initial steps in the MCM-catalyzed reaction. (a) The stepwise pathway, which is the generally accepted pathway for AdoCbl activation, occurs in two steps: (I) homolytic cleavage of the Co−C5′ bond of dAdoCbl yields cob(II)alamin and 5′-deoxyadenosyl radical (dAdo•) and (II) H-atom abstraction from methylmalonyl-CoA by dAdo• forms dAdo−H plus a substrate-derived radical. In the alternative concerted pathway, cleavage of the Co−C5′ bond and H-atom abstraction occur simultaneously, without the intermediacy of a distinct dAdo• species. (b) Inset: the active-site residues described quantum-mechanically (except for Gln330) in this study.

is known that the Co−C5′ homolysis is kinetically coupled to the H-atom-transfer step[23] and is associated with a large primary deuterium isotope effect, which is indicative of quantum mechanical tunneling.[24]

Further, recent ultrafast photolysis experiments have provided direct spectroscopic evidence for the existence of dAdo• in the active sites of the dAdoCbl-dependent enzymes glutamate mutase (GM)[25,26] and ethanolamine ammonia lyase (EAL).[27−29] The formation of dAdo• (from dAdoCbl) has also been well characterized in solution.[30,31] Additional evidence for the participation of dAdo• in enzymatic H-atom transfer reactions is also found within the superfamily of radical *S*-adenosylmethionine (SAM) enzymes.[32,33] Here, dAdo• is formed by reductive cleavage of the C−S bond of SAM by an $[Fe-4S]^{+1}$ cluster, which also produces methionine.

Despite the extensive experimental evidence in favor of a stepwise mechanism, recent computational investigations of the AdoCbl-dependent systems have yielded conflicting mechanistic conclusions. For example, the conductor hypothesis, which proposes an explicit role for cob(II)alamin in the stabilization of the radical intermediates involved in H-atom transfer,[34] was investigated by density functional theory (DFT) calculations. In a gas-phase model relevant to GM, this work identified a concerted Co−C5′ cleavage and H-atom-abstraction pathway (Figure 1a), that is stabilized by ∼30 kJ mol^{-1} relative to one that is stepwise.[35] However, a subsequent study, also in the gas-phase, found that the existence of either pathway is determined by the initial configuration of the ribose moiety of dAdoCbl relative to the corrin ring, rather than an inherent preference for one pathway over the other.[36] Interestingly, an interaction between the unique C19−H

dx.doi.org/10.1021/ja207809b | *J. Am. Chem.Soc.* 2012, 134, 1591−1599

bond of the corrin ring and the O3′ of the ribose moiety was observed in this context. While this interaction appeared to provide stabilization for the Co−C5′ cleavage in these models, it was uncertain whether such observations would remain relevant in the enzyme.

On the other hand, quantum mechanics/molecular mechanics (QM/MM)[37,38] ONIOM(DFT/MM) calculations have provided support for a stepwise mechanism[39,40] and identified a potential energy minimum corresponding to the dAdo• intermediate. Furthermore, attempts to locate a concerted transition structure in the protein environment were unsuccessful and the results indicated that the energy for H-atom transfer rises sharply as the Co−C5′ distance is decreased. The results of an earlier QM/MM study of Co−C5′ cleavage of dAdoCbl in GM were also consistent with a stepwise pathway in the protein environment.[41] These QM/MM investigations also carefully examined the various energetic contributions to the catalytic reduction of the Co−C5′ cleavage barrier. Although the total magnitudes of the reductions and the detailed decompositions differed somewhat between these studies, the analyses concluded that the energy contributions could be divided among a cage effect (∼20 kJ mol^{-1}), a protein-coenzyme effect (ranging between ∼40 and ∼70 kJ mol^{-1}), and a ground-state destabilization or strain effect of the coenzyme (ranging between ∼25 and ∼60 kJ mol^{-1}).

Warshel and co-workers examined the MCM-catalyzed reaction using a dynamical approach based on an EVB/MM description.[42] Their calculations identified a concerted pathway for the Co−C5′ cleavage and H-atom abstraction. With the introduction of extensive configurational sampling, they found no evidence for a minimum on the free-energy surface corresponding to the dAdo• intermediate. These authors argued against the previously identified strain contribution, suggesting that it was an artifact of the minimization procedures and concluded that the catalysis arises through an electrostatic stabilization of the transition state geometry. This rationalization is in line with the traditional view of enzyme catalysis, as understood in the context of transition state theory (TST).[43]

Taken together, it appears that there is still no consensus from a theoretical point of view as to the details of the generation and control of the dAdo• radical within the enzyme, despite a number of impressively thorough computational studies. The gas-phase studies[35,36] favor either concerted or stepwise Co−C5′ homolysis and H-atom-transfer mechanisms, depending on the approach used. Even though such approaches can provide fundamental insights at a modest computational cost,[44] they may lack structural motifs relevant to catalysis. The QM/MM studies,[39−41] which do include the protein environment, argue for the existence of a potential energy minimum for dAdo• as part of a stepwise mechanism and identify strain as an important element of catalysis. However, in the absence of configurational sampling these approaches do not probe the free energy surface or the dynamics of the intermediate. The only dynamical study,[42] which did include the effects of configurational sampling and finite temperature,[45] found the catalysis to be primarily of an electrostatic nature, in the context of a concerted mechanism, with no distinct intermediate on the free energy surface. However, it has been pointed out that the predictive nature of the EVB calculations employed in that study may be compromised because of their inherent parametrization with experimental data and DFT.[46] In particular, parametrization against B3-LYP may be especially problematic in this case as that functional is known to perform poorly for cobalamin species.[47]

To provide fresh insights into these complex issues, we have used first-principles (Car−Parrinello)[48] molecular dynamics (MD) simulations within a QM/MM framework[49] to investigate the initial stages of the MCM-catalyzed reaction (Figure 1a). This methodology offers distinct advantages over the previous studies because it allows the free energy, and hence the catalysis, to be computed from first principles using DFT. Simultaneously, the actual dynamics of the dAdo• radical and the related aspects of the enzymatic control of reactive intermediates can be examined in this same framework. The price one has to pay for these advantages is that long simulations become prohibitively expensive. However, as detailed below, a number of measures have been taken to try to ensure that all simulations in the present work are adequately converged.

COMPUTATIONAL METHODS

Structural Model and Classical MD Simulations. The MCM crystallographic structure (PDB entry code 4REQ) was used in all calculations.[12] The system was solvated with TIP3P water molecules[50] in a rectangular box of dimensions 125 × 125 × 98 Å^3, and sodium counterions were added to neutralize the system, which included approximately 140 000 atoms, including ca. 40 000 water molecules. The AMBER ff03 force field[51] was used to represent the MM region in the classical and QM/MM simulations. Parameters for cob(II)alamin, 5′-deoxyadenosine, and methylmalonyl-CoA were derived in a manner consistent with the standard AMBER protocol for a state in which the Co−C5′ bond was broken (as in 4REQ). This protocol, the RESP charges, atom types, and additional force field parameters are presented in Table S1. The protonation state of His244 was determined by carrying out three MD and three QM/MM MD simulations with different initial protonation states. Based on these simulations, the epsilon form of His244 was adopted, since only the simulated structures with His244 in this form were found to be in good agreement with the crystal structure (rmsd <0.7 Å for the active-site heavy atoms).

Force-Field-Based MD Simulations. The system was treated within full periodic boundary conditions. Electrostatic interactions were computed with the smooth particle-mesh Ewald (SPME) algorithm[52] with a cutoff of 10 Å for both the real-space part of the electrostatic interactions and the van der Waals term. A preliminary step involved geometry optimization of the full structure by use of the conjugate-gradient algorithm. Energy minimization was carried out in two steps, first with harmonic restraints on the MCM protein active site, followed by minimizations without any restraints.

MD simulations were conducted with restraints on the protein backbone atoms at constant volume (NVT ensemble), increasing the temperature from 0 to 300 K in five steps, for a total of 50 ps. The last restrained configuration at 300 K was then used to start the unrestrained constant pressure constant temperature (NPT ensemble) equilibration for 100 ps. Finally, an MD production run of ∼5 ns at constant pressure (1 atm) and temperature (300 K) was performed to provide starting configurations for the subsequent QM/MM calculations. All of the classical simulations used an integration time step of 1.5 fs. The temperature control of the simulations was achieved by coupling the system to a Berendsen thermostat.[53] All classical simulations were performed with the AMBER 8 suite of programs.[54]

QM/MM Simulations. QM/MM MD simulations were carried out using CPMD 3.13[55] and the QM/MM scheme of the Röthlisberger group.[49] The QM region was treated with the BP86 functional[56,57] with a plane-wave cutoff of 70 Ry and included the corrin ring, the 5′-deoxyadenosyl group bound to the cobalt atom, His244, Glu370, and part of the substrate, in line with a previous study[58] (Figure 1b). Core electrons for Co, C, O, and N atoms were described using semicore Martins and Trouiller pseudopotentials,[59] with nonlocal corrections for Co. The adequacy of BP86 to describe the structural and electronic

dx.doi.org/10.1021/ja207809b | J. Am. Chem.Soc. 2012, 134, 1591−1599

properties of cobalamins has been reported previously.[47,60] Hydrogen atoms were used to close the valences of the QM system. The QM box size was 22 × 22 × 22 Å^3 and contained 208 atoms. Car–Parrinello QM/MM simulations[49] were performed at 300 K with a Nosé-Hoover chain of thermostats[61] using a coupling constant of 700 cm^{-1}. The electron fictitious mass was set at 400 au.

After a suitable equilibration period for a structure extracted from the classical simulations in which the Co–C5′ bond was cleaved, we performed a steered QM/MM simulation to gradually form the Co–C bond over a period of 10 ps.

Free Energy Calculations. Thermodynamic integration using constrained MD (CMD) was employed to estimate the energy requirements (potential of mean force, PMF) of the Co–C5′ bond cleavage and H-atom-transfer steps. Constraints were employed so that the reaction coordinate remained fixed at a given value. The Co–C distance was sampled every 0.1 Å between 2.0 and 5.0 Å. Well-equilibrated initial coordinates for each constrained simulation were generated from snapshots extracted from the aforementioned steered MD trajectory. At each Co–C5′ separation, constrained QM/MM simulations were then performed for 1.5 ps per point at 300 K. The first ∼0.5 ps were used for equilibration, while the remainder of the time was used for analysis. In Figure S1, we demonstrate by progressively increasing the sampling times that the average forces (and hence the reaction free energy barrier) are satisfactorily converged. The absence of slow motions required to obtain a converged PMF curve was assessed by performing enhanced sampling with the accelerated ab initio MD method.[62] Further, the mean constraint force with respect to the reaction coordinate was determined by integration in both the forward and reverse directions, and the overall hysteresis effects were found to be small, indicating that the relevant degrees of freedom of the system have been fully sampled.

Similar protocols were implemented to compute the free energy profile for the H-atom abstraction. In this case, an epsilon coordinate, defined as $\varepsilon = [r(\text{Sub:C–Sub:H})] - [r(\text{dAdo:C5′–Sub:H})]$, where Sub is the substrate and dAdo is the 5′-deoxyadenosyl radical, was used. The appropriateness of the ε and Co–C5′ collective variables (CVs) was tested with CMD by computing the mean force for chosen values of ε and Co–C5′, and different initial coordinates. The consistent agreement between the forces suggests that coordinates orthogonal to the CVs are adequately sampled during the simulations, and implies that the two CVs can describe accurately the chemical transformations. CMD simulations were run for 17 values of ε (−3.00, −2.50, −2.00, −1.75, −1.50, −1.25, −1.00, −0.75, −0.50, −0.25, 0.0, 0.25, 0.50, 0.75, 1.00, 1.50, and 2.00) to obtain the free energy profile for the H-atom-abstraction step.

Metadynamics (MTD) was used to examine both Co–C5′ cleavage and H-atom abstraction in a single trajectory in order to provide information about the overall free energy of the process. MTD was performed in two dimensions using ε (see above) and Co–C5′ as CVs. Gaussian functions were added to the potential every 50 MD steps (∼5 fs), where 0.3 Å and 3.7 kJ mol^{-1} were chosen as the half-width and depth of the gaussians, respectively. The free energy surface for dAdoCbl (Figure 2b) was obtained from 20 ps of sampling (see the Supporting Information for an error estimate). The free energy surfaces for 2′-ddAdoCbl and 3′-ddAdoCbl (Figure S5) were obtained from 5 ps runs and are only intended to provide qualitative support for the other results.

RESULTS AND DISCUSSION

Free Energy Calculations Reveal the Existence of the dAdo$^\bullet$ Radical Intermediate. We begin by presenting simulations of the Co–C5′ cleavage and H-atom-abstraction processes, starting from a model of MCM that incorporates an intact Co–C5′ bond with an equilibrium distance of 2.05 Å. The PMF for Co–C5′ cleavage was evaluated from a series of QM/MM simulations with constrained values of the Co–C5′ coordinate. The resulting average constraint forces were integrated to yield the free energy profile[63] (see Computational Methods for details). The results, shown in Figure 2a, indicate that the free energy rises sharply as the bond is elongated. The highest point occurs at a Co–C5′ distance of 3.60 Å, corresponding to a barrier for the Co–C5′ bond cleavage of 63.9 ± 3.2 kJ mol^{-1}. This result compares favorably with estimates obtained from kinetics experiments, which indicate a barrier of 54.8 ± 2.5 kJ mol^{-1}.[9] The slight overestimate of the barrier is consistent with results in previous studies of cobalamins with the BP86 functional.[60]

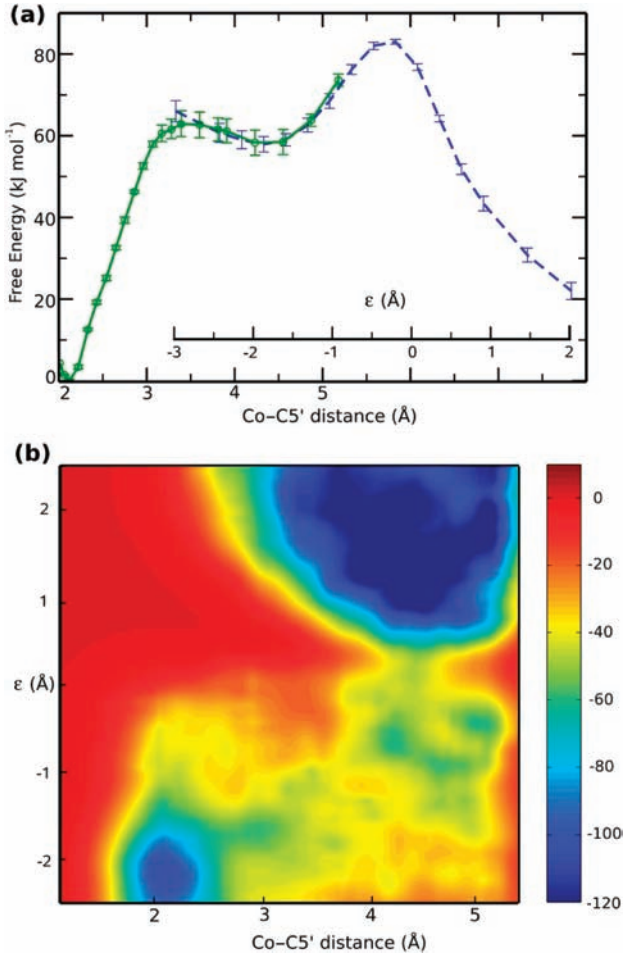

Figure 2. Free energy profiles (kJ mol^{-1}) for the Co–C5′ bond homolysis (green solid line) and H-atom abstraction (blue dashed line) steps, indicative of a stepwise pathway. (a) Constrained MD was performed along the Co–C5′ bond distance and an H-abstraction coordinate (ε). (b) 2D free energy surface computed with metadynamics.

Although it is difficult to decompose a free energy barrier obtained from CMD into enthalpic and entropic components, experimental investigations indicate that the Co–C activation in this case is dominated by an enthalpic contribution (91%).[4] This result does not, however, obviate the need for a dynamical approach to avoid problems associated with multiple minima on the potential energy surface and finite temperature effects.[64]

Despite the good agreement between the CMD free energy barrier and experiment, we were encouraged to consider an intriguing mechanism for Co–C cleavage that has recently been suggested by Kozlowski, Yoshizawa and co-workers.[65,66] Their proposal entails the deprotonation of Tyr89 by the carboxylate (COO$^-$) of the substrate to generate a Tyr–O$^-$ anion, which could potentially transfer an electron to AdoCbl and facilitate

dx.doi.org/10.1021/ja207809b | J. Am. Chem.Soc. 2012, 134, 1591–1599

the Co−C5′ bond scission. To test this possibility, we temporarily expanded our QM region to include the side chain of Tyr89. However, simulations with a neutral side chain (Tyr−OH) did not exhibit any spontaneous proton transfer to the substrate COO^- moiety. On the other hand, during simulations that began with a neutral carboxylic acid group (COOH) and a deprotonated tyrosine ($Tyr-O^-$), spontaneous proton transfer between these groups was observed, within a few bond vibrations. This result is consistent with the nominal pK_a values of the carboxylic acid group (∼4) and tyrosine (∼10). These data, together with the good agreement with experimental data for the computed Co−C5′ cleavage barrier (obtained with Tyr−OH), led us not to pursue this possibility further.

The free energy profile shown in Figure 2a displays a minimum between Co−C5′ distances of 4.0 and 4.5 Å, which in our simulations corresponds to the free dAdo• radical. To investigate the H-abstraction step, a second PMF curve was computed along a standard transfer coordinate (ε, see Computational Methods). Relative to dAdo•, the barrier for H-atom transfer is found to be 25.2 ± 5.1 kJ mol^{-1}. In total, the energy requirements for the stepwise pathway are 81.5 ± 6.0 kJ mol^{-1}.

Bearing in mind that our use of two independent coordinates (Co−C5′ and ε) may introduce a bias toward a stepwise result, we have constructed a 2D free energy surface along both coordinates using MTD,[67] which is free from any such bias. The appropriateness of these two coordinates, and the sampling times used, were determined after extensive testing (see Computational Methods and SI for details). In Figure 2b, the lowest energy pathway can be seen to be comprised of two steps. Starting in the lower left-hand corner with the intact coenzyme, it is clear that the most favorable reaction coordinate proceeds toward the lower right-hand corner of the graph, as the Co−C5′ bond is extended, with no significant change in the ε coordinate. At long Co−C5′ bond lengths, a free energy basin, corresponding to the dAdo• radical, can be clearly discerned. Barrier-crossing events in the ε direction from this basin are only likely to occur when large Co−C5′ distances are attained. The MTD results are thus entirely consistent with a stepwise pathway for MCM (Figure 2a).

The free energy barriers for Co−C5′ cleavage and H-atom abstraction on the MTD surface are predicted to be 64.5 ± 2.5 and 24.5 ± 2.5 kJ mol^{-1}, respectively. We note that these results compare well with those from the individual PMFs (Figure 2a, 63.9 ± 3.2 and 25.2 ± 5.1 kJ mol^{-1}, respectively). Concerted pathways that do not involve the creation of a dAdo• intermediate are found to lie at least 20 kJ mol^{-1} higher in free energy. These results thus serve to justify the description of the 2D reaction surface by two sequential 1D coordinates, as shown in Figure 2a. They also demonstrate the existence of the elusive dAdo• radical intermediate on a first-principles free energy surface.

Controlling the Diffusion of the dAdo• Radical Intermediate. More than 20 years ago, Rétey advanced the idea that the dAdoCbl-dependent enzymes function, in part, to create a high energy dAdo• intermediate that undergoes controlled diffusion toward the substrate from which it can abstract a hydrogen atom.[68] The principal role of the protein in this model is to ensure strict control over the motion of dAdo• within the confines of the active site so as to prevent unwanted side-reactions. This so-called "negative catalysis" continues to be somewhat controversial today as it can be considered to be at odds with the much more established transition-state stabilization model.

Our calculations indicate that dAdo• is associated with a clear minimum on the free energy surface (Figure 2). The barrier for re-formation of the Co−C5′ bond is, however, small (∼5−10 kJ mol^{-1}) compared with the barrier for H-abstraction (∼20−25 kJ mol^{-1}). Thus, under these conditions, dAdo• could be predominantly expected to recombine with cob(II)alamin, and only a very small proportion of trajectories would be productive.

To examine further the time scale of the radical diffusion, we have performed a series of unbiased simulations of dAdo• in the enzyme, starting from selected structures extracted along the Co−C5′ coordinate. At short Co···C5′ separations, such as 3.40 Å (SI, Figure S4), we observe the Co−C5′ bond to re-form within 1 ps, which is consistent with the low recombination barrier. However, at longer initial Co···C5′ separations (e.g., 3.65 Å), we instead observe that dAdo• diffuses toward the substrate and, within a few ps, reaches a free energy minimum (Figure 3a and Figure S3) in a position in close contact with the substrate. Our simulations indicate that the dAdo• radical is fully formed and stable in such a minimum for at least 20 ps (Figure 3b). Over this time, the Co−C5′ bond of dAdoCbl neither re-formed nor did dAdo• abstract an H atom from the substrate. Similar behavior was observed consistently during five additional unconstrained simulations that started from Co···C5′ separations larger than 3.6 Å. These results suggest that the active site of the enzyme is structured in such a way that the lifetime of the intermediate is sufficiently prolonged to increase the chances for productive H-abstraction by selectively positioning the reactive carbon atom dAdo• close to the substrate methyl group.

In the context of a simplistic TST picture, the H-abstraction would be expected to occur in ∼2 ns (which corresponds to an effective barrier of ca. 25 kJ mol^{-1}). This time scale, however, would be shortened in the presence of quantum mechanical tunneling of the H-atom,[24] which is not accounted for by the classical nuclear treatment within the CPMD approach that we have employed in the present study. In this context, a previous QM/MM study of MCM found that tunneling may increase the rate of H-atom transfer by one to two orders of magnitude.[69] This estimate was obtained assuming a stepwise pathway and produced excellent agreement between the calculated kinetic isotope effects and those obtained from experiment. Combining our own simulations with these considerations, we expect the lifetime of dAdo• at 300 K to be between about 20 and 200 ps, and certainly less than 2 ns. Although this is short enough to explain the difficulties associated with the experimental observation of dAdo• in the enzymatic environment, it is sufficiently long to suggest that sophisticated ultrafast techniques could indeed yield a positive result in the context of thermolytic enzyme turnover.

The apparent adoption of a stable active-site conformation by dAdo• also serves to protect it from unwanted side reactions, both with species within the enzyme cavity as well as in the surrounding medium. This picture is entirely consistent with Rétey's negative catalysis concept, where the role of the protein is not simply to lower energy barriers, but also to impart controlled selectivity to the highly reactive dAdo• intermediate.

Importance of the Ribose Hydroxyl Groups. The major catalytic effect of the coenzyme B_{12}-dependent enzymes is believed to be the ca. 70 kJ mol^{-1} reduction in the barrier for Co−C5′ bond cleavage.[9] For this reason, we have monitored

dx.doi.org/10.1021/ja207809b | J. Am. Chem.Soc. 2012, 134, 1591−1599

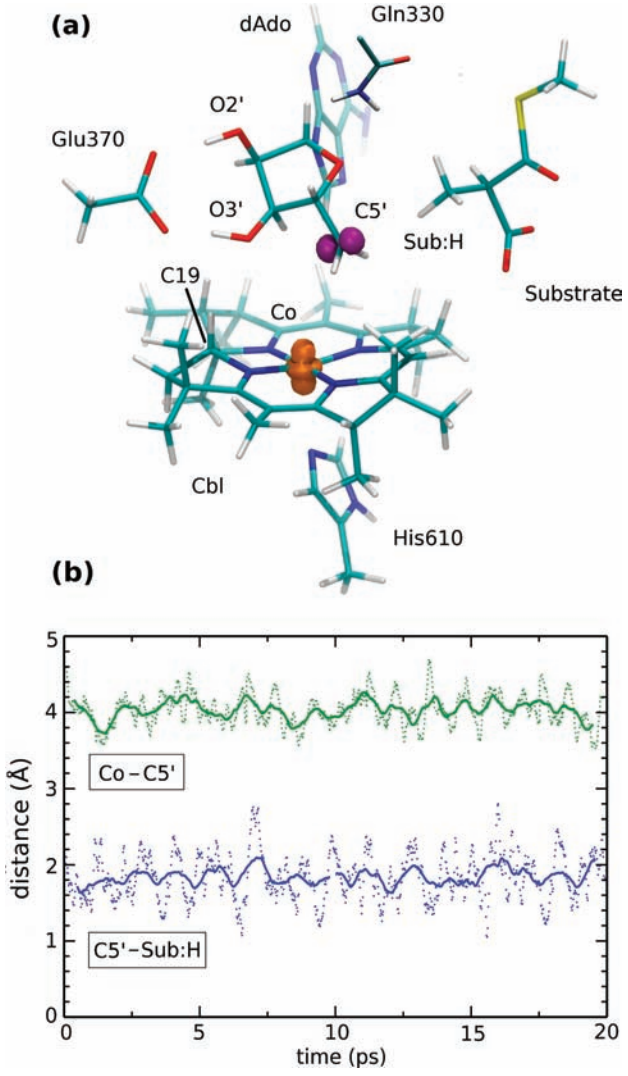

Figure 3. Unconstrained QM/MM MD trajectories of the dAdo• radical. These correspond to the sampling of a minimum on the free energy surface located next to the substrate of MCM. (a) The spin density of dAdo• and cob(II)alamin at long Co···C5′ separation. (b) Bond distances shown as time series.

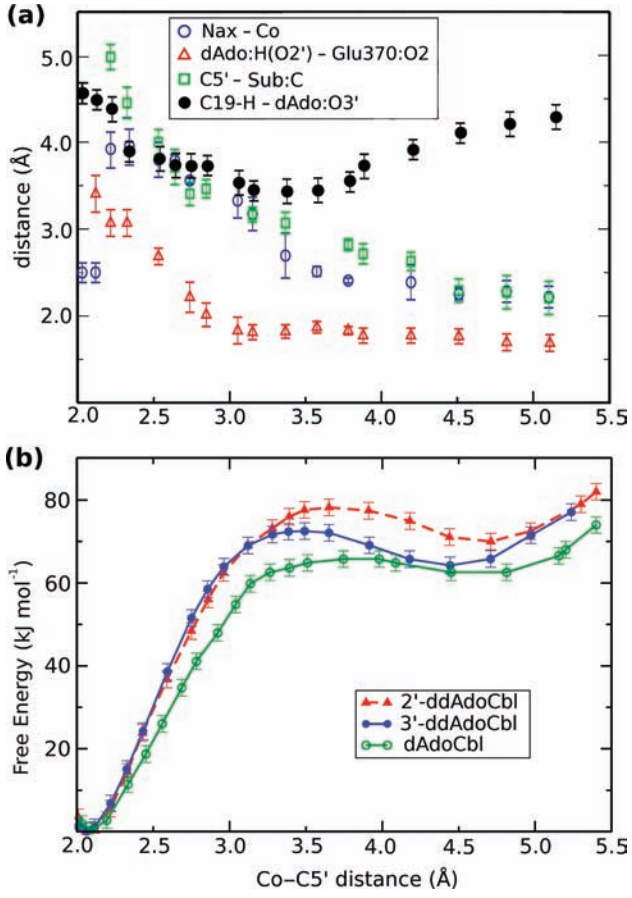

Figure 4. Selected structural and free energy changes that occur in dAdoCbl as the Co–C5′ bond is lengthened. (a) Equilibrium values at fixed Co–C5′ distances. (b) PMFs of the Co–C5′ bond cleavage in dAdoCbl, 2′-ddAdoCbl, and 3′-ddAdoCbl.

selected structural rearrangements and interactions that took place during our simulations of this phase of the reaction (Figure 4a). We begin our discussion with parameters related to the two ribose OH groups of the dAdoCbl cofactor. Of particular interest is our finding that the distance between dAdo:H(O2′) and Glu370:O2 decreases rapidly as the Co–C5′ bond breaks (Figure 4a). In contrast, the distance between dAdo:O3′ and Glu370:O1 varies to a relatively small extent during the same phase of the reaction (see Movie S1). Once the distance between dAdo:H(O2′) and Glu370:O2 has reached an optimal value of ∼1.6 Å, it remains roughly constant during the subsequent diffusion of dAdo• toward the substrate (cf. Figure 4a). Interestingly, we observe a marked shortening of the distance between dAdo:O3′ and the unique C19–H moiety of cobalamin, which occurs only as the Co–C5′ bond is being broken.

To further probe the importance of the ribose OH groups, we have investigated analogs of dAdoCbl in which either the 2′-OH or 3′-OH group has been replaced by an H atom (Figures 4b, S5b, and S5c). For 2′,5′-dideoxyadenosylcobalamin (2′-ddAdoCbl), we again find the cleavage and abstraction reactions to occur in a stepwise fashion with a distinct intermediate on the free energy surface (Figures 4b and S5b). In the absence of the 2′-OH group, there is a significantly reduced attraction of dAdo:O2′ toward Glu370 during the Co–C5′ cleavage, which results in a ca. 15 kJ mol^{-1} increase in the barrier (to 78.4 ± 2.3 kJ mol^{-1}, Figure 4b, triangles). These results are consistent with an earlier experimental study in which the incubation of MCM with 2′-ddAdoCbl resulted in only 1–2% enzyme activity.[70] At that time, it was farsightedly hypothesized that the 2′-OH group of dAdoCbl participates in stabilizing the initially formed radicals (i.e., dAdo• and cob(II)alamin). Taken together with other studies,[39−42] these data suggest that Glu370 helps to catalyze the reaction, predominantly through its interaction with the 2′-OH group of dAdoCbl, by stabilizing the cleavage products following Co–C5′ homolysis (Figure 4a).

With the goal of quantifying the energetic magnitude of the interaction between dAdo:O3′ and C19–H, we also characterized the reaction in the presence of 3′,5′-dideoxyadenosylcobalamin (3′-ddAdoCbl). In this case, the Co–C5′ cleavage barrier is increased by ca. 10 kJ mol^{-1} (to 72.5 ± 2.2 kJ mol^{-1}, Figure 4b, filled circles) relative to dAdoCbl, suggesting that the activity of MCM with 3′-ddAdoCbl is likely to be greater than the activity observed with 2′-ddAdoCbl but less than that observed with dAdoCbl. Moreover, given that the deeper well associated with 3′-ddAdo• (Figures 4b and S5c) would be

dx.doi.org/10.1021/ja207809b | J. Am. Chem.Soc. 2012, 134, 1591–1599

expected to increase the lifetime of this intermediate, further experimental investigation of this analog may be warranted. Our results also indicate that O3′ is important for catalysis and that cob(II)alamin may well play a small but important role in stabilizing dAdo•, in accordance with the conductor hypothesis,[34] through the interaction between O3′ and C19−H.[36] However, the magnitude of this stabilization appears to be somewhat less in the enzymatic environment than in the gas phase.[35,36]

Other Catalytic Interactions. It is interesting to note that we observe a pseudorotation in the ribose conformation for the natural cofactor that occurs as the Co−C5′ bond is breaking, which is partly driven by the previously mentioned interaction between dAdo:O3′ and C19−H (Figure 5a, Movie S1). This

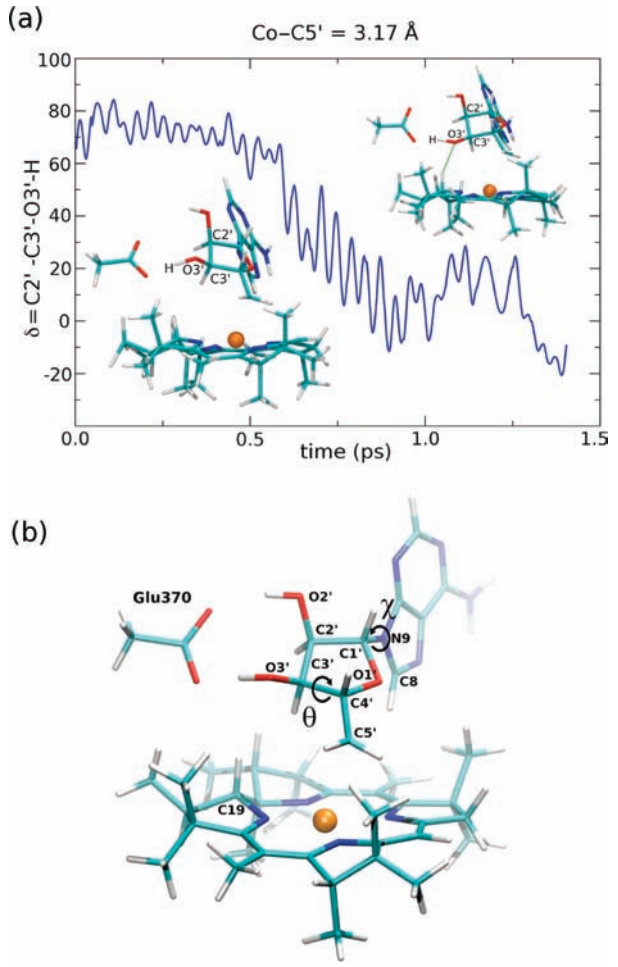

Figure 5. (a) Pseudorotation of the ribose ring highlighting the importance of sampling. The interaction of O3′ of Ado• with the unique C19−H moiety of cobalamin is possible only once the Co−C5′ bond is extended, at Co−C5′ distances between 3.0 to 4.0 Å, but is only observed after 0.5 to 1 ps. (b) The numbering system for the ribose.

pseudorotation, which appears to be similar to that observed in X-ray structures of the related enzyme glutamate mutase,[71] enables H-bonding between dAdo:O1′ and a side-chain amide proton of Gln330 (see Figure 3a). An important result of this rearrangement is the correct positioning of the radical center with respect to the substrate (Figures 3a and 4a). Interestingly, when the Co−C5′ PMF for dAdoCbl is integrated using the constraint force that is measured before the occurrence of this pseudorotation, the resulting energy profile is some 15 kJ mol^{-1} higher than that shown in Figure 2a. In this sense, the specific interactions involving the two ribose hydroxyl groups, the apical oxygen and the accompanying pseudorotation appear to be responsible not only for reducing the Co−C5′ cleavage barrier by up to 40 kJ mol^{-1} but also for the directed diffusion of the dAdo• intermediate toward the substrate.

The lower axial His610 ligand also appears to participate in the Co−C5′ cleavage, as suggested by the mutagenesis experiments of Banerjee et al., which provided an upper bound of ca. 15 kJ mol^{-1} for its contribution to the catalysis.[72] As the Co−C5′ distance is initially increased, the Co−N_{ax} distance extends from 2.3 to ∼4.0 Å (Figure 4a), a phenomenon termed the inverse trans effect.[73] Following this initial period, which involves the formation of a hydrogen bond between the delta nitrogen of His610 and Asp608, the axial ligand then returns to interact with cobalt at Co−C5′ distances >3.5 Å (Movie S1). During this process, the cobalt atom, which is slightly above the corrin ring plane initially, moves downward toward His610 as the Co−C5′ bond starts to break (Figure S6a). The cobalt atom then returns into the plane of the corrin ring once the Co−C5′ bond is broken (∼3.5 Å) and eventually moves under the corrin ring (by ca. ∼0.1 Å) to optimize its interaction with His610. Consistent with this observed behavior, out-of-plane displacements of Co have been suggested to occur in the active site of MCM in the presence and absence of substrate analogs.[74] Further, this action may assist in preventing the re-formation of the Co−C5′ bond and serve an important biological function by reducing the recrossing rate.

The geometric parameters of the ribose ring have often been used to argue for steric destabilization of the intact coenzyme as an important contributor to catalysis. One such parameter is the Co−C5′−C4′ angle (see Figure 5b), which is found to adopt an initial value of 133 ± 5° in our simulations. The fact that this angle is larger than the optimal gas-phase value (124°) has been interpreted as evidence that high strain energy is stored in the ribose.[47] We also observe in our simulations that the ribose ring adopts a less stable, eclipsed conformation (as evidenced by the C1′−C2′−C3′−C4′ dihedral angle) at Co−C5′ distances between 2.6 and 2.8 Å. This allows dAdo• to optimize both the Co−C5′ interaction and the electrostatic interactions involving Glu370 with the ribose OH groups, albeit at the expense of choosing a slightly less stable ribose conformation. While this might be viewed as steric destabilization,[39−41] it has been argued that this "strain energy" arises only so as to enable the favorable electrostatic interaction of Glu370 with the ribose.[42] Our present free energy calculations are consistent with this view and indicate that the catalytic effect originates primarily from defined (electrostatic) interactions within the active site.

■ CONCLUDING REMARKS

We have carried out a QM/MM simulation study of the mechanism of radical generation and transfer in the reaction catalyzed by the dAdoCbl-dependent enzyme methylmalonyl-CoA mutase (MCM). Our calculations provide strong evidence that the dAdo• radical lies at a minimum on the free energy surface and thus corresponds to a distinct intermediate in the enzymatic environment. We have been able to witness the motion of the dAdo• radical in the enzyme as it diffuses, in a controlled manner, toward the substrate. This movement is initiated by a pseudorotation of the ribose, which is assisted by

the two ribose OH groups. The removal of either the 2′-OH or 3′-OH group from dAdoCbl disrupts the interaction between dAdo• and the enzyme. Taken together, these data suggest that the two "polar handles" of the ribose play a dual role in the catalytic process, as they facilitate both the Co−C5′ cleavage and assist the radical diffusion.

Our methodology also allows us to describe several correlated motions, involving active-site residues such as Gln330, Glu370, His610, and Asp608, which are important for catalysis. These few specific interactions are primarily of an electrostatic nature and contribute of the order of 55 kJ mol^{-1} to the catalysis of cofactor activation. Their importance appears to vary as the Co−C5′ bond is cleaved and the dAdo• intermediate diffuses toward the substrate. As a result, the lifetime of dAdo• in the active site appears to have been optimized to increase the probability of H-abstraction. A similar radical-shuttling mechanism almost certainly applies to other class I dAdoCbl-dependent enzymes, such as glutamate mutase.[71]

Our proposed mechanism is in the spirit of Rétey's negative catalysis,[68] where the role of the protein is not simply to lower energy barriers, but also to manipulate the highly reactive radical intermediate. It is also compatible with a recent time-resolved spectroscopic study, which found that concepts such as ground-state destabilization or the "switching" to a specific protein conformation, designed to stabilize the intermediate state (dAdo•), were not compatible with measurements on the enzyme EAL.[28] Instead, the data were more compatible with a continuous, protein-based stabilization along the reaction coordinate, of the type described herein (see, Movie S1). Finally, our results are also consistent with contemporary ideas that enzyme specificity can be controlled through multiple, consecutive steps.[75,76] A similar dual strategy could be proposed in the design of new nanodevices at the interface between biology and technology.

■ ASSOCIATED CONTENT

Supporting Information

Full citation for ref 54, Supplementary Text S1, Supplementary Figures S1 to S6, Supplementary Table S1, and Movie S1. This material is available free of charge via the Internet at http://pubs.acs.org.

■ AUTHOR INFORMATION

Corresponding Author

*bucher.denis@gmail.com; gmsandala@gmail.com; radom@chem.usyd.edu.au; david.smith@irb.hr

Present Address

⊥Department of Chemistry and Biochemistry, University of California, San Diego, La Jolla, California 92093, U.S.A.

■ ACKNOWLEDGMENTS

We gratefully acknowledge funding (to L.R.) from the Australian Research Council, the award (to G.M.S.) of an NZZ Fellowship (02.03/63), the award (to D.B.) of a postdoctoral fellowship from the Swiss Science Foundation, support (to D.M.S.) provided by the MSES (098-0982933-2937) and EAM-FAU (Excellence Cluster), and generous computing grants (to L.R.) from the NCI National Facility and Intersect Australia Ltd.

■ REFERENCES

(1) *Chemistry and Biochemistry of B_{12}*; Banerjee, R., Ed.; Wiley-Interscience: New York, 1999.
(2) Banerjee, R. *Biochemistry* **2001**, *40*, 6191−6198.
(3) Reed, G. H. *Curr. Opin. Chem. Biol.* **2004**, *8*, 477−483.
(4) Brown, K. L. *Chem. Rev.* **2005**, *105*, 2075−2149.
(5) Frey, P. A.; Hegeman, A. D.; Reed, G. H. *Chem. Rev.* **2006**, *106*, 3302−3316.
(6) Marsh, E. N. *Biochem. Soc. Trans.* **2009**, *37*, 336−342.
(7) Gruber, K.; Puffer, B.; Kräutler, B. *Chem. Soc. Rev.* **2011**, *40*, 4346−4363.
(8) Halpern, J. *Science* **1985**, *227*, 869−875.
(9) Chowdhury, S.; Banerjee, R. *Biochemistry* **2000**, *39*, 7998−8006.
(10) Zhang, W.; Shaikh, A. U.; Tsui, E. Y.; Swager, T. M. *Chem. Mater.* **2009**, *21*, 3234−3241.
(11) Mancia, F.; Keep, N. H.; Nakagawa, A.; Leadlay, P. F.; McSweeney, S.; Rasmussen, B.; Bösecke, P.; Diat, O.; Evans, P. R. *Structure* **1996**, *4*, 339−350.
(12) Mancia, F.; Evans, P. R. *Structure* **1998**, *6*, 711−720.
(13) See, for example: Banerjee, R. *Chem. Rev.* **2003**, *103*, 2083−2094.
(14) Chandler, R. J.; Venditti, C. P. *Mol. Genet. Metab.* **2005**, *86*, 34−43.
(15) Gaudemer, A.; Zylber, J.; Zylber, N.; Baran-Marszac, M.; Hull., W. E.; Fountoulakis, M.; Konig, A.; Wolfle, K.; Rétey, J. *Eur. J. Biochem.* **1981**, *119*, 279−285.
(16) Chen, D.; Abend, A.; Stubbe, J.; Frey, P. A. *Biochemistry* **2003**, *42*, 4578−4584.
(17) Mansoorabadi, S. O.; Padmakumar, R.; Fazliddinova, N.; Vlasie, M.; Banerjee, R.; Reed, G. H. *Biochemistry* **2005**, *44*, 3153−3158.
(18) Bothe, H.; Darley, D. J.; Albracht, S. P.; Gerfen, G. J.; Golding, B. T.; Buckel, W. *Biochemistry* **1998**, *37*, 4105−4113.
(19) Pierik, A. J.; Ciceri, D.; Lopez, R. F.; Kroll, F.; Bröker, G.; Beatrix, B.; Buckel, W.; Golding, B. T. *Biochemistry* **2005**, *44*, 10541−10551.
(20) Bender, G.; Poyner, R. R.; Reed, G. H. *Biochemistry* **2008**, *47*, 11360−11366.
(21) Magnusson, O. Th.; Frey, P. A. *J. Am. Chem. Soc.* **2000**, *122*, 8807−8813.
(22) Mansoorabadi, S. O.; Magnusson, O. Th.; Poyner, R. P.; Frey, P. A.; Reed, G. H. *Biochemistry* **2006**, *45*, 14362−14370.
(23) Padmakumar, R.; Padmakumar, R.; Banerjee, R. *Biochemistry* **1997**, *36*, 3713−3718.
(24) Chowdhury, S.; Banerjee, R. *J. Am. Chem. Soc.* **2000**, *122*, 5417−5418.
(25) Sension, R. J.; Cole, A. G.; Harris, A. D.; Fox, C. C.; Woodbury, N. W.; Lin, S.; Marsh, E. N. G. *J. Am. Chem. Soc.* **2004**, *126*, 1598−1599.
(26) Sension, R. J.; Harris, D. A.; Stickrath, A.; Cole, A. G.; Fox, C. C.; Marsh, E. N. G. *J. Phys. Chem. B* **2005**, *109*, 18146−18152.
(27) Robertson, W. D.; Warncke, K. *Biochemistry* **2009**, *48*, 140−147.
(28) Robertson, W. D.; Wang, M.; Warncke, K. *J. Am. Chem. Soc.* **2011**, *133*, 6968−6977.
(29) Jones, A. R.; Hardman, S. J. O.; Hay, S.; Scrutton, N. S. *Angew. Chem., Int. Ed. Engl.* **2011**, *50*, 10843−10846.
(30) Bussandri, A. P.; Kiarie, C. K.; van Willigen, H. *Res. Chem. Intermed.* **2002**, *28*, 697−710.
(31) Cole, A. G.; Yoder, L. M.; Shiang, J. J.; Anderson, N. A.; Walker, L. A.; Holl, M. M. B.; Sension, R. J. *J. Am. Chem. Soc.* **2002**, *124*, 434−441.
(32) Frey, P. A.; Hegeman, A. D.; Ruzicka, F. J. *Crit. Rev. Biochem. Mol. Biol.* **2008**, *43*, 63−88.
(33) Marsh, E. N. G.; Patterson, D. P.; Li, L. *ChemBioChem* **2010**, *11*, 604−621.
(34) Buckel, W.; Kratky, C.; Golding, B. T. *Chem.—Eur. J.* **2005**, *12*, 352−362.
(35) Kozlowski, P. M.; Kamachi, T.; Toraya, T.; Yoshizawa, K. *Angew. Chem., Int. Ed. Engl.* **2007**, *46*, 980−983.

(36) Durbeej, B.; Sandala, G. M.; Bucher, D.; Smith, D. M.; Radom, L. *Chem.—Eur. J.* **2009**, *15*, 8578−8585.
(37) Warshel, A.; Levitt, M. *J. Mol. Biol.* **1976**, *103*, 227−249.
(38) For a recent review,see: Senn, H. M.; Thiel, W. *Angew. Chem., Int. Ed. Engl.* **2009**, *48*, 1198−1229.
(39) Kwiecien, R. A.; Khavrutskii, I. V.; Musaev, D. G.; Morokuma, K.; Banerjee, R.; Paneth, P. *J. Am. Chem. Soc.* **2006**, *128*, 1287−1292.
(40) Li, X.; Chung, L. W.; Paneth, P.; Morokuma, K. *J. Am. Chem. Soc.* **2009**, *131*, 5115−5125.
(41) Jensen, K. P.; Ryde, U. *J. Am. Chem. Soc.* **2005**, *127*, 9117−9128.
(42) Sharma, P. K.; Chu, Z. T.; Olsson, M. H. M.; Warshel, A. *Proc. Natl. Acad. Sci. U.S.A.* **2007**, *104*, 9661−9666.
(43) Truhlar, D. G.; Garrett, B. C.; Klippenstein, S. J. *J. Phys. Chem.* **1996**, *100*, 12771−12800.
(44) See, for example: Sandala, G. M.; Smith, D. M.; Radom, L. *Acc. Chem. Res.* **2010**, *43*, 642−651.
(45) Warshel, A. *Annu. Rev. Biophys. Biomol. Struct.* **2003**, *32*, 425−443.
(46) Jensen, K. P.; Ryde, U. *Coord. Chem. Rev.* **2009**, *253*, 769−778.
(47) Jensen, K. P.; Ryde, U. *J. Phys. Chem. A* **2003**, *107*, 7539−7545.
(48) Car, R.; Parrinello, M. *Phys. Rev. Lett.* **1985**, *55*, 2471−2474.
(49) Laio, A.; VandeVondele, J.; Rothlisberger, U. *J. Chem. Phys.* **2002**, *116*, 6941−6947.
(50) Jorgensen, W. L.; Chandrasekhar, J.; Madura, J.; Impey, R. W.; Klein, M. L. *J. Chem. Phys.* **1983**, *79*, 926−935.
(51) Duan, Y.; Wu, C.; Chowdhury, S.; Lee, M. C.; Xiong, G.; Zhang, W.; Yang, R.; Cieplak, P.; Luo, R.; Lee, T.; Caldwell, J.; Wang, J.; Kollman, P. *J. Comput. Chem.* **2003**, *24*, 1999−2012.
(52) Essmann, U.; Perera, L.; Berkowitz, M. L.; Darden, T.; Lee, H.; Pedersen, L. G. *J. Chem. Phys.* **2003**, *103*, 8577−8593.
(53) Berendsen, H. J. C.; Postma, J. P. M; Van Gunsteren, W. F.; Dinola, A.; Haak, J. R. *J. Chem. Phys.* **1984**, *81*, 3684−3690.
(54) Case, D. A; et al. AMBER 8, University of California: San Francisco, CA, 2004.
(55) CPMD, http://www.cpmd.org.
(56) Becke, A. D. *Phys. Rev. A* **1998**, *38*, 3098−3100.
(57) Perdew, J. P. *Phys. Rev. B* **1986**, *33*, 8822−8824.
(58) Kozlowski, P. M.; Kuta, J.; Galezowski, W. J. *Phys. Chem. B* **2007**, *111*, 7638−7645.
(59) Troullier, N.; Martins, J. L. *Phys. Rev. B* **1991**, *43*, 1993−2006.
(60) Kuta, J.; Patchkovskii, S.; Zgierski, M. Z.; Kozlowski, P. M. *J. Comput. Chem.* **2006**, *27*, 1429−1437.
(61) Martyna, G. J.; Klein, M. L.; Tuckerman, M. *J. Chem. Phys.* **1992**, *97*, 2635−2643.
(62) Bucher, D.; Pierce, L. C. T.; McCammon, J. A.; Markwick, P. R. *J. Chem. Theory Comput.* **2011**, *7*, 890−897.
(63) Carter, E. A.; Ciccotti, G.; Hynes, J. T.; Kapral, R. *Chem. Phys. Lett.* **1989**, *156*, 472−477.
(64) Klähn, M.; Braun-Sand, S.; Rosta, E.; Warshel, A. *J. Phys. Chem. B* **2005**, *109*, 15645−15650.
(65) Kumar, M.; Kozlowski, P. M. *J. Phys. Chem. B* **2009**, *113*, 9050−9054.
(66) Kozlowski, P. M.; Kamachi, T.; Kumar, M.; Nakayama, T.; Yoshizawa, K. *J. Phys. Chem. B* **2010**, *114*, 5928−5939.
(67) Laio, A.; Parrinello, M. *Proc. Natl. Acad. Sci. U.S.A.* **2002**, *99*, 12562−12566.
(68) Rétey, J. *Angew. Chem. Intl. Ed. Engl.* **1990**, *29*, 355−361.
(69) Dybala-Defratyka, A.; Paneth, P.; Banerjee, R.; Truhlar, D. *Proc. Natl. Acad. Sci. U.S.A.* **2007**, *104*, 10774−10779.
(70) Calafat, A. M.; Taoka, S.; Puckett, J. M. Jr.; Semerad, C.; Yan, H.; Luo, L.; Chen, H.; Banerjee, R.; Marzilli, L. G. *Biochemistry* **1995**, *34*, 14125−14130.
(71) Gruber, K.; Reitzer, R; Kratky, C. *Angew. Chem., Int. Ed. Engl.* **2001**, *40*, 3377−3380.
(72) Vlasie, M.; Chowdhury, S.; Banerjee, R. *J. Biol. Chem.* **2002**, *277*, 18523−18527.
(73) Kuta, J.; Wuerges, J.; Randaccio, L.; Kozlowski, P. M. *J. Phys. Chem. A* **2009**, *113*, 11604−11612.
(74) Brooks, A. J.; Vlasie, M.; Banerjee, R.; Brunold, T. C. *J. Am. Chem. Soc.* **2005**, *127*, 16522−16528.
(75) Ma, B. Y.; Nussinov, R. *Curr. Opin. Chem. Biol.* **2010**, *14*, 652−659.
(76) Kamerlin, S. C. L.; Warshel, A. *Prot. Struct. Funct. Bioinfo.* **2010**, *78*, 1339−1375.